

# 16QAM Wireless Communication Model

M. Meenaakumari

*A. Abstract---* Software defined radio (SDR) has emerged as a priority theme of research since it will substitute for conventional implementation on wireless communication system. In this paper, a multi-standards SDR model is designed and implemented in FPGA form using Xilinx system generator technique. According to the under sampling theory which is used in this model, the received 70MHz carrier is sampled at 40MHz and the performance of the proposed model with different standards' like GSM, OFDM, and WCDMA using 16QAM modem is produced attractive behavior with different channel effective and minimum BER. Therefore make develop on 3G of wireless and mobile systems more economical, effective and accelerate the transition from 3G to 4G of wireless systems.

**Keywords:** SDR, FPGA, Wireless Communications.

---

## I. INTRODUCTION

Field-programmable gate arrays (FPGAs) are widely used to implement physical layer signal processing functions for software-defined radios (SDRs [1] [2]). FPGAs provide very high performance custom hardware solutions, and can be reconfigured in system, and when bringing up a new waveform in the modem. Despite their reprogrammability, they have historically been considered part of the “hardware” within a modem, rather than part of the “software”. Consequently, the SDR software control layer, or Software communications Architecture (SCA [3]), has largely ignored issues related to the specification, configuration, signal transport, or inter-component interfaces that are important to the platform provider of an SDR that exploits FPGAs. Wireless communication networks have become more popular in the past two decades since the advent of cellular communications. The rapid growth in cellular communications has proved that wireless communication is viable for voice and data services. Traditional wireless devices are designed to deliver a single communication service using a particular standard [4]. With the steady increase of new wireless services and standards, single purpose devices with dedicated hardware resources can no longer meet the user's needs. It is also expensive to upgrade and maintain a wireless system each time a new standard comes into existence. A feasible solution to make communication systems more flexible and user friendly can be achieved through the software defined radio (SDR) concept. Software defined radio refers to the class of reprogrammable or reconfigurable radios in which the same piece of hardware can perform different functions at different times [5].

## II. SYSTEM MODEL FOR IMPLEMENTATION

Simulation of the SDR system with SIMULINK tools forms is the first step of the design process for reconfigurable computing. For an exact representation of the FPGA implementation, the Xilinx system generator block set in MATLAB is used. The complete simulink SDR model show in Fig (1) and the parameters of proposal model are given in table (1).

---

M. Meenaakumari, Assistant Professor, Department of Electronics and Communication Engineering, BIST, BIHER, Bharath Institute of Higher Education & Research, Selaiyur, Chennai. E-mail: meenumathi.m@gmail.com

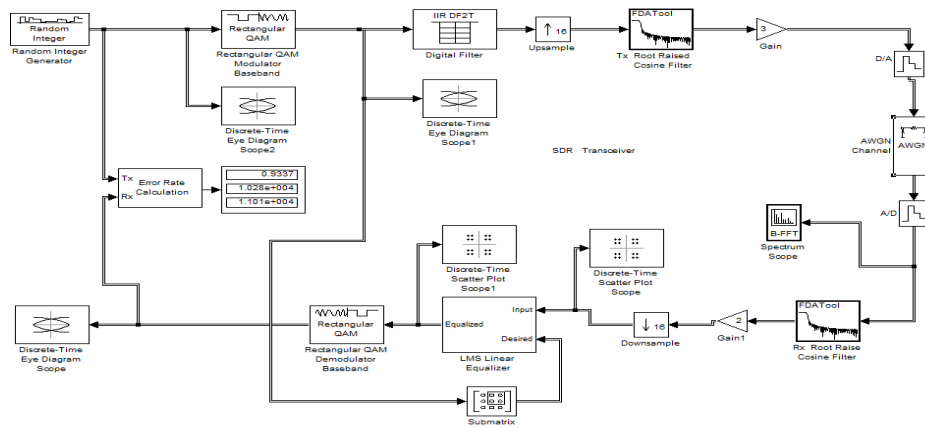


Figure 1: proposed SDR transceiver model.

Table 1: Simulation Parameters of Proposed Model

Modulation Type	16QAM
Symbol Rate	2.5Msymbol/Second
Interpolation Factor	16
Channel Model	AWGN
Receiver Sampling Rate	40 MHz
IF	70MHz

### III. SYSTEM GENERATOR BASED DESIGN FLOW

Simulation and testing of the transceiver design flow were done using *System Generator*, a system level modeling tool from Xilinx [6]. This tool can be used for designing and testing DSP systems for FPGAs in a visual data flow environment such as MATLAB *Simulink*. The *System Generator* based design flow [7] is shown figure (2). The system model is created in the MATLAB environment using Xilinxlibrary. This diagram shows one of three ways to design a system. This is a typical design flow for HDL Co-Simulation. This diagram shows that we can use Black Box and include user’s VHDL code or IP core along with Xilinx System Generator’s blocks in the design and generate a synthesizable design which can be implemented using Xilinx ISE’s Project Navigator. It also uses ModelSim block which is a helper block to invoke ModelSim simulator and actually simulate the design. The simulator’s output is fed back to Simulink and the results can be displayed using Simulink’s sinks.

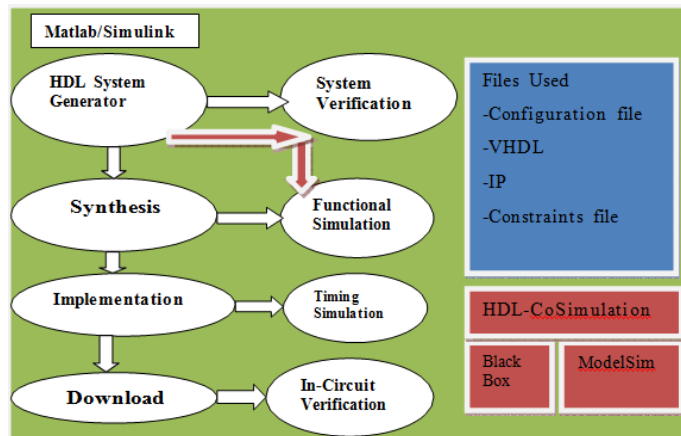
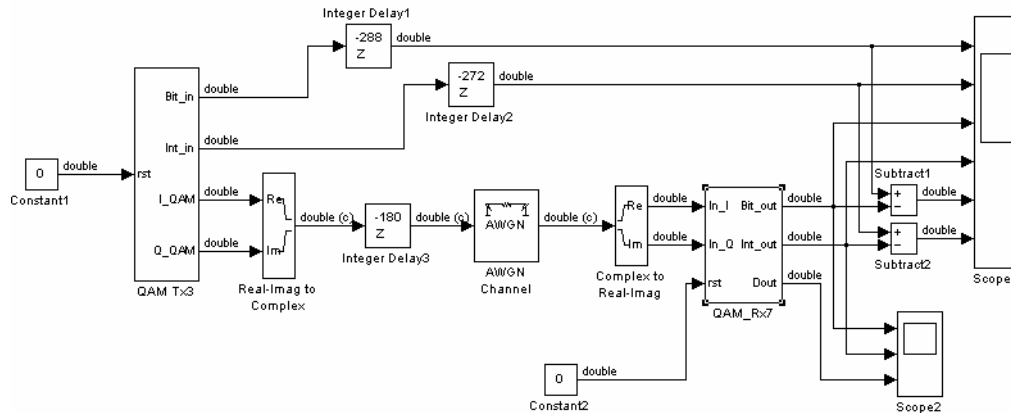


Figure 2: System Generator based design flow (Xilinx Inc., 2003).

### System Generator Design

The goal of our implementation is to mimic an ideal SDR based 16QAM communication system. Quadrature Amplitude Modulation, QAM, has fast become the dominant modulation mechanism for high speed digital signals. From the wireless 802.11 protocols to ADSL modems to personal communicators for the military, QAM has become a necessary part of our daily lives. With increases in processing power, QAM as a part of software defined radio (SDR) schema is now easily achievable. This section details a System generator implementation of 16-QAM communication system in FPGA which would be suitable for a SDR system. Figure (3) shows a high level SDR transceiver.



**Figure 3:** 16-QAM transceiver using system generator

The implementation can be broken down into three main stages: transmitter, channel and receiver. The modulation and demodulation stages are comprised of several distinct subsystems.

#### 4.1. Transmitter

In the transmitter, the baseband signal is generated using programmable digital signal processing techniques. The generated signal is 16QAM with a symbol rate  $2.5Msymbol/sec$ . The transmitter part show in figure (4) and the constellation -eye diagram of the generated baseband signal show in fig.(5).

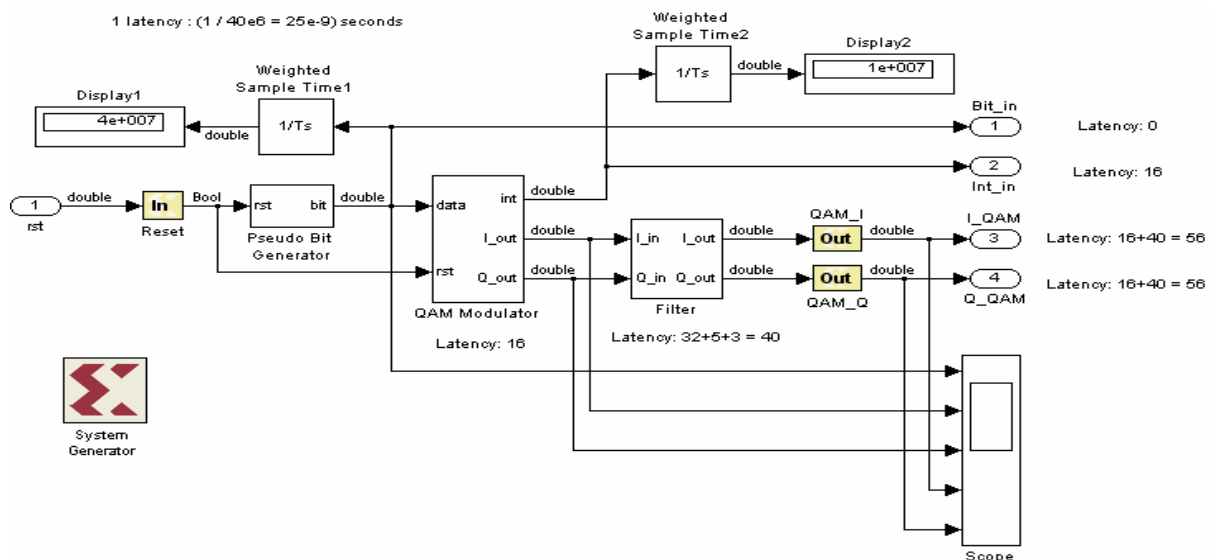


**Figure 4:** 16-QAM Transmitter (QAM Tx3 subsystem) using System Generator.

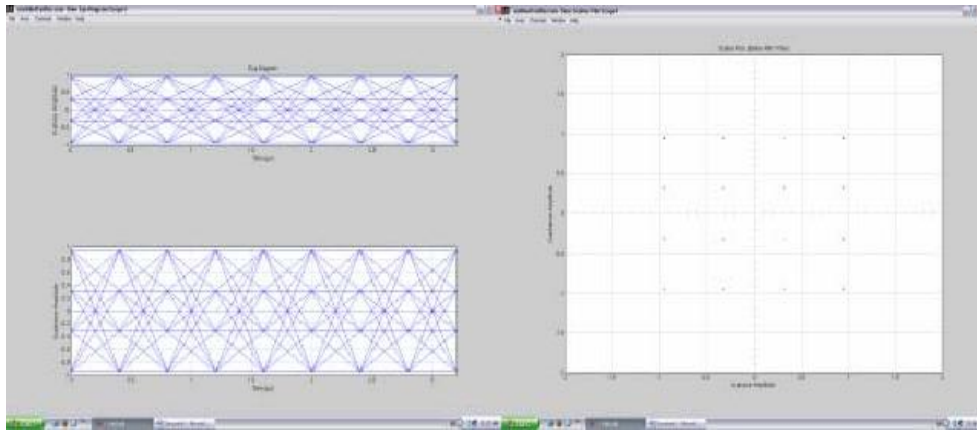


**Figure 5:** Generated Baseband Signal: (a) eye diagram, (b) constellation diagram.

The input and output signals for transmitter part is show in figure (6). As show from signals the input bit of 10Mbps was modulated first and transferred to 2.5Msps 16QAM baseband (IQ) signal. The signal is then passed through a channel distortion filter to show the effect of ISI in the system. After that, the signal is passed through pulse shaping filter (root raised cosin filter) to limit the transmitted bandwidth. Finally, it is up-converted to IF using NCO (Numerically Controlled Oscillator). The final stage is the IF-to-RF conversion which is typically implemented in the analog domain.

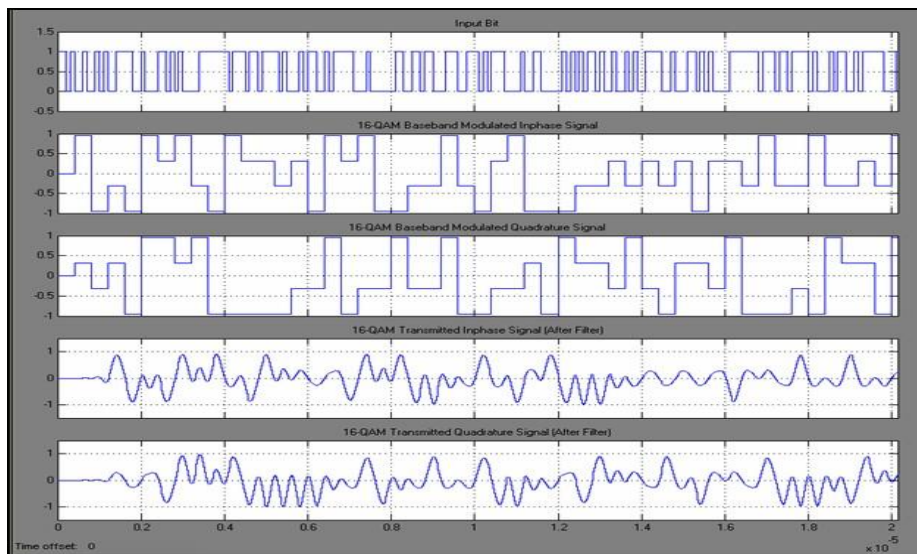


**Figure 6:** Transmitted Signal: Input bit = 10 Mbps, (16-QAM Baseband Modulated (IQ) signal = 2.5Msps), (16-QAM Transmitted (IQ) signal =  $16 \times 2.5 = 40$  Msps (16 bit, 13 fractional length)).

#### 4.2. Channel

The transmission channel has several effects on the signal in a physical system. The finite bandwidth of the channel will cause distortion in the ideal signal, noise from various sources will also be introduced and finally the channel may also attenuate the input signal. Other effects, such as dispersion, may also be present. The effects of attenuation and noise can be modelled by adding Gaussian white noise to the signal, effectively changing the signal to noise ratio present at the receiver. The effects of finite bandwidth can be modelled by a simple filter. The original power spectrum of baseband transmitted signal is show infig.(7).

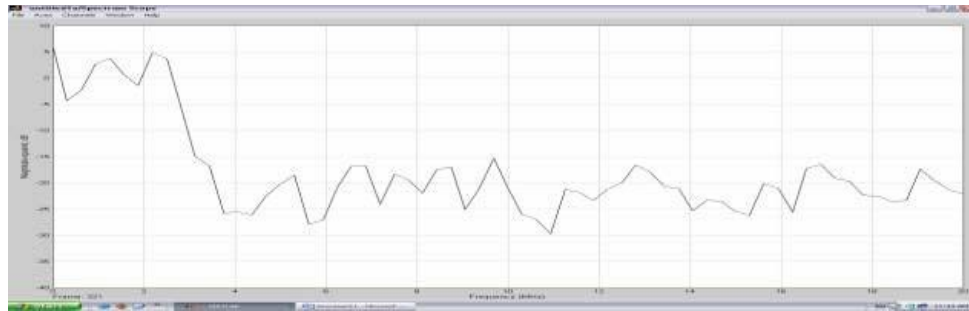


**Figure 7:** power Spectrum of Original Baseband Signal.

### 4.3. Receiver

In the receiver, after the signal is contaminated by noise, it down converted to IF and then sampled and processed using programmable digital signal processing techniques. The IF input signal is at 70MHz while the sampling frequency used in the proposed receiver model is 40MHz so, under-sampling technique plays the main role in the receiver stage. A fundamental part of many communication systems is the digital down converter. This allows a signal to be shifted from its carrier (or IF) frequency down to baseband. The sampled IF signal is down converted to its baseband through a digital down converter (DDC) works by first shifting the bandwidth of interest to baseband by multiplying the received signal by a close approximation to the original carrier. This work is based on the simplified mathematical principle. There is a technique known as bandpass sampling used to sample a continuous bandpass signal that is centered about some frequency other than zero HZ. When a continuous input signal's bandwidth and center frequency permit us to do so, bandpass sampling not only reduces the speed requirement of A/D converters below that necessary with traditional low-pass sampling; it also reduces the amount of digital memory necessary to capture a given time interval of a continuous signal. The demodulation section is by far the most complicated part of the QAM model. The demodulator must detect the phase and amplitude of the signal, decode the symbol based on the phase and amplitude and then finally convert the data back to a serial stream. In order to complete the symbol demodulation, recovery of the symbol clock is required. Figure (8) shows the receiver system generator block. The constellation and eye diagram of received baseband 16QAM signal is show in fig.(9).

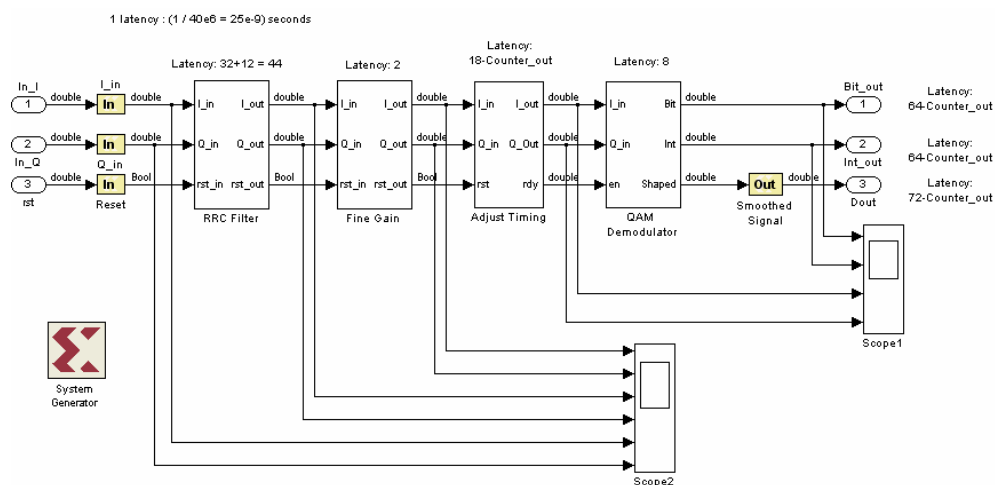


**Figure 8:** Receiver part of 16-QAM (QAM Rx7 subsystem) using System Generator.

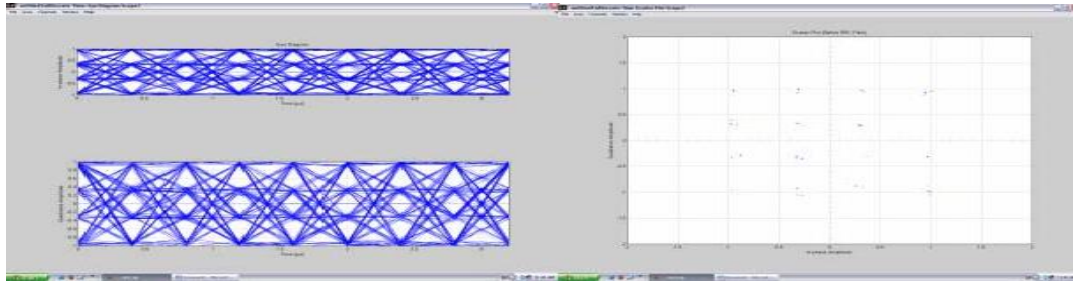


**Figure 9:** 16QAM baseband received signal: (a) eye diagram, (b) constellation diagram.

It is obvious from eye diagram the effect of inter-symbol interference as the eye is nearly closed. And from the constellation diagram, the received signal suffers from phase error due to noise and channel distortion. In order to solve this problem, an adaptive equalizer (variable taps coefficients using LMS Algorithm) is used to improve the system performance and reduce the error in phase. This is clearly shown in Fig.(10) which represents the constellation diagram of signal before and after equalization.

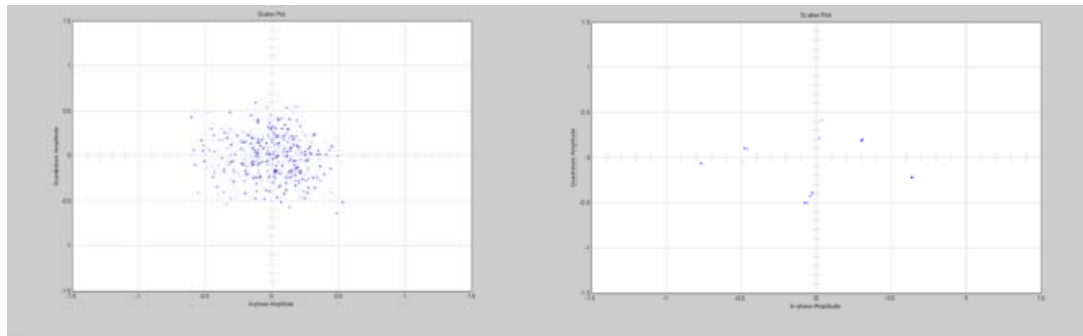


**Figure 10:** Constellation diagram of the received baseband signal (a) before equalizer, (b) after Equalization.

The input and output signals for receiver part is show in figure (11),(12).

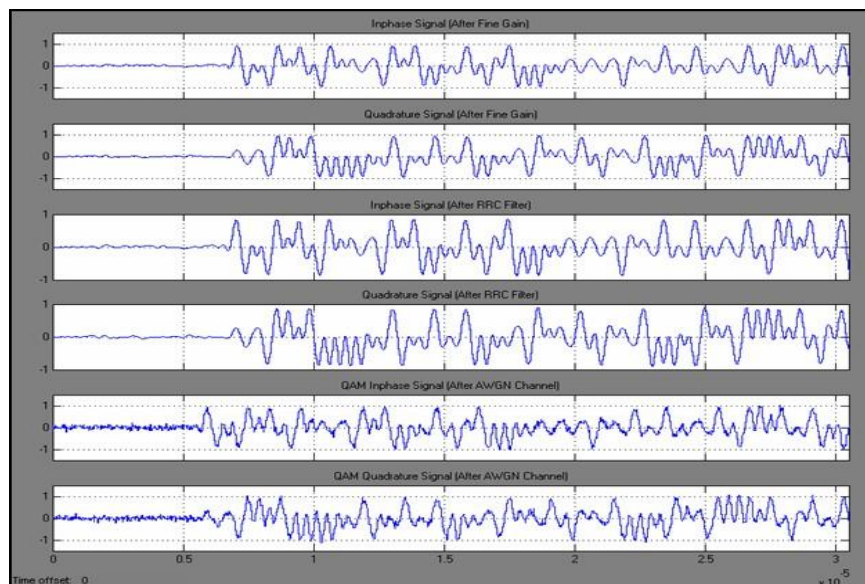


**Figure 11:** Receiver Signal



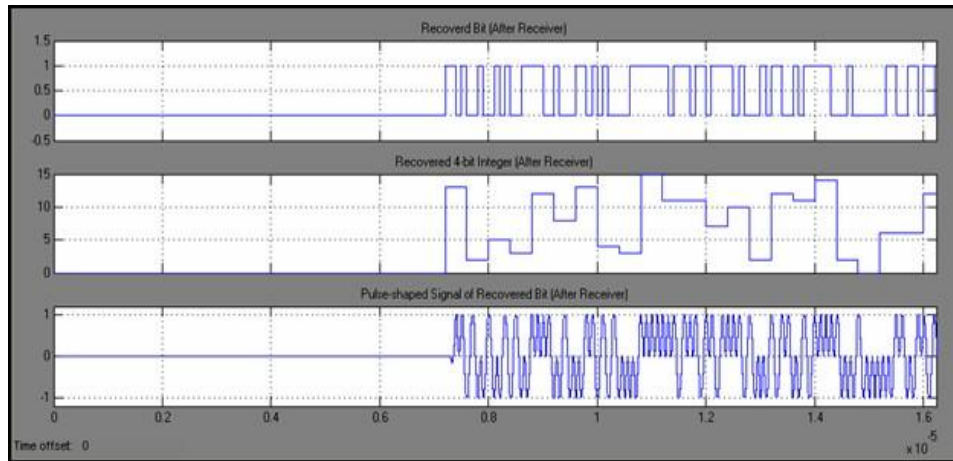


**Figure 12:** Receiver Output Signal: Recovered 4-bit Integer = 5 Msps, Recovered bit:  $2.5 \times 4 = 10$  Mbps, Pulse-shaped signal of Recovered bit:  $10 \times 8 = 80$  Msps (16 bit, 14 fractional length).

#### 4.4. Timing Recovery

In any QAM scheme timing recovery poses a significant problem for the recovery of a quality signal. A wide variety of methods are available for timing recovery, however, their usefulness actually depends on the type of transmitted data. The simulation software will be using a Bernoulli coded random bit sequence so none of the decision based schemes would have an advantage. In this case the best choice would be a synchroniser timing recovery circuit. To reduce complexity, a simple times-two timing recovery system was implemented. After a significant amount of tuning, the timing recovery still had a significant amount of jitter. As expected, the jitter was dependent on the data being transmitted. Directed timing recovery as the best recovery scheme for random signals as show in fig(13).

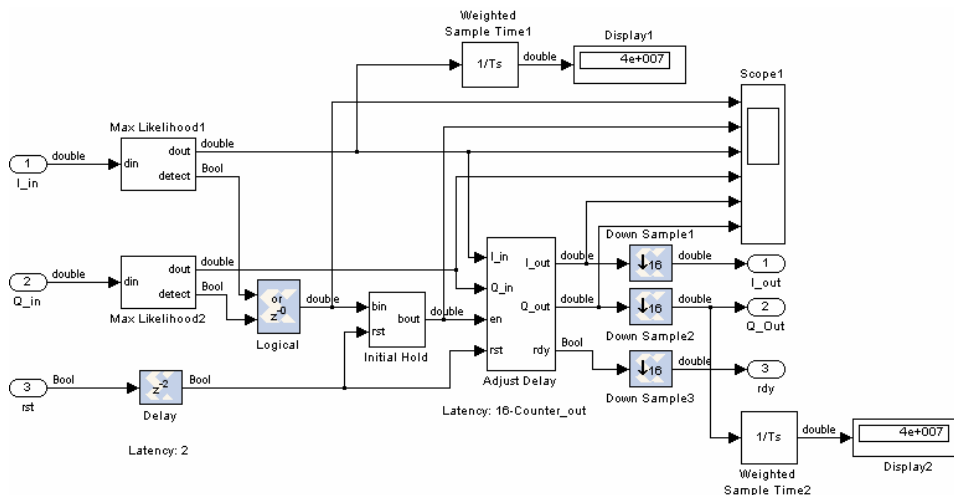


**Figure 13:** Timing Recovery (Adjust Timing subsystem in QAM Rx7)

#### 4.5. FPGA Implementation Results

The final step in our design is to download the system generator model HDL cod to the FPGA form Virtex-4 using Xilinx system generator program. In this paper the transmitter part of the SDR system is implemented in FPGA Virtex-4 board number (1) using the HDL code of system generator, which is used to analyze the system. The

receiver part of SDR system is implemented in FPGA Virtex-4 board number (2). Fig.(14) show the Physical Assembly of SDR transceiver.

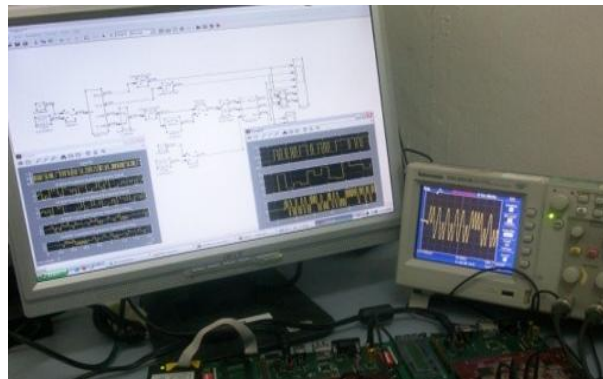


**Figure 14:** Physical Assembly of SDR transceiver

The details of transmit and received IQ signal is show in figs.(15),(16) and (17).

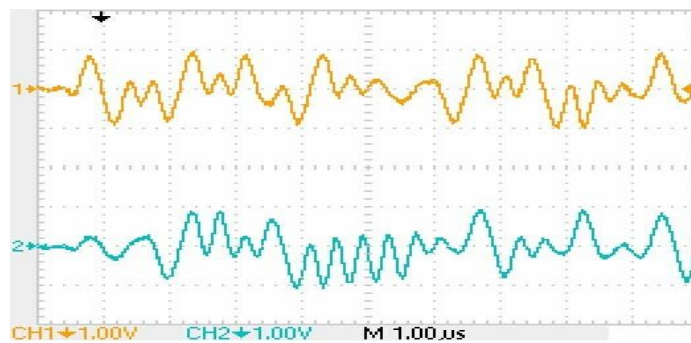


**Figure 15:** transmitted (IQ) QAM signals from DAC

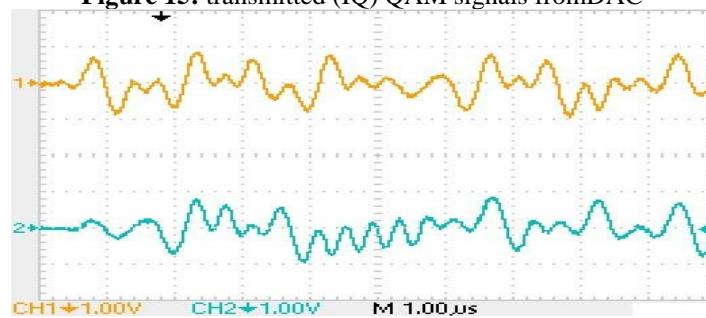


**Figure 16:** receiver IQ signal Filtered by RRCfilter.

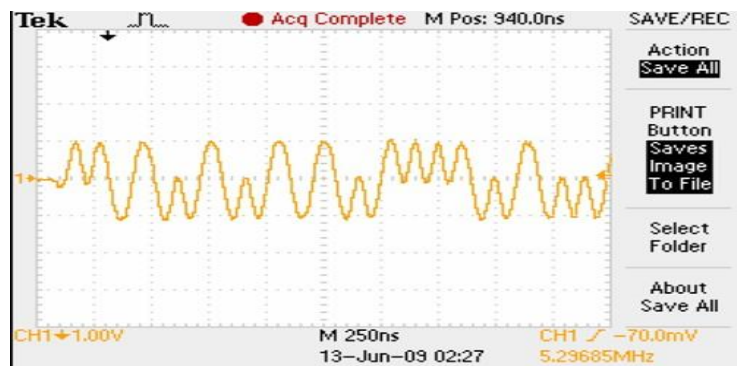


**Figure 17:** output signal of receiver FPGA after DAC.



#### IV. CONCLUSION

In this paper the design of Software Defined Radio (SDR) model is present. For the design of SDR model in Matlab/Simulink, the transmitted signal with 2.5 MHz bandwidth undergoes 20 dB SNR (Signal-to-Noise Ratio) in Additive White Gaussian Noise (AWGN) channel between transmitter and receiver. The similarity of demodulated output data in receiver and input data of transmitter in integers (10 Mbps) shows the communication between transmitter and receiver is successful, although bit (data) error may occur. For the design of SDR model in System Generator, Pseudo Noise Generator module is used to generate 10 Mbps random bits as transmitter input data. In receiver part, Adjust Timing module is required to recover symbol timing for optimum sampling point for the following demodulation process. The demodulated output data in receiver is pulse-shaping of the reconstructed bits because 50 ohm transmission line transformer after DAC in P240 Analog Module does not allow DC (direct current) signal to flow through it, despite the demodulated output is reconstructed bit in ideal case of receiver in SDR model. However, the AWGN channel is also 20 dB SNR for 2.5 MHz bandwidth signal transmission between transmitter and receiver. Both the real-time (empirical) and simulated results for transmitted signal and receiver output in time domain shows equivalence in shape although there are some minor differences due to limitation of the 50 ohm transmission line transformer after DAC in P240 Analog Module. The equivalence also proves the bit-true and cycle-true of the FPGA processing which are important in high speed DSP for further processing of pre-coding, decoding and equalization in more advanced SDR model. Therefore this develop on 3G of wireless and mobile systems more economical, effective and accelerate the transition from 3G to 4G of wireless systems.

#### REFERENCES

- [1] Sakthipriya N., An effective method for crop monitoring using wireless sensor network, Middle - East Journal of Scientific Research, V-20, I-9, PP:1127-1132, 2014.
- [2] Vijayaragavan S.P., Karthik B., Kiran Kumar T.V.U., Effective routing technique based on decision logic for open faults in fpgas interconnects, Middle - East Journal of Scientific Research, V-20, I-7, PP:808-811, 2014.
- [3] Kanniga E., Selvamaratham K., Sundararajan M., Kandigital bike operating system, Middle - East Journal of Scientific Research, V-20, I-6, PP:685-688, 2014.
- [4] Sundararajan M., Optical instrument for correlative analysis of human ECG and breathing signal, International Journal of Biomedical Engineering and Technology, V-6, I-4, PP:350-362, 2011.
- [5] Khanaa V., Thooyamani K.P., Saravanan T., Simulation of an all optical full adder using optical switch, Indian Journal of Science and Technology, V-6, I-SUPPL.6, PP:4733-4736, 2013.
- [6] Slimani Y., Baykal A., Amir M., Tashkandi N., Güngüneş H., Guner S., El Sayed H.S., Aldakheel F., Saleh T.A., Manikandan A., Substitution effect of Cr<sup>3+</sup> on hyperfine interactions, magnetic and optical properties of Sr-hexaferrites, Ceramics International, V-44, I-13, PP:15995-16004, 2018.
- [7] Suguna S., Shankar S., Jaganathan S.K., Manikandan A., Novel Synthesis of Spinel Mn<sub>x</sub>Co<sub>1-x</sub>Al<sub>2</sub>O<sub>4</sub> (x = 0.0 to 1.0) Nanocatalysts: Effect of Mn<sup>2+</sup> Doping on Structural, Morphological, and Opto-Magnetic Properties, Journal of Superconductivity and Novel Magnetism, V-30, I-3, PP:691-699, 2017.
- [8] Mathubala G., Manikandan A., Arul Antony S., Ramar P., Enhanced photocatalytic activity of spinel Cu<sub>x</sub>Mn<sub>1-x</sub>Fe<sub>2</sub>O<sub>4</sub> nanocatalysts for the degradation of methylene blue dye and opto-magnetic properties, Nanoscience and Nanotechnology Letters, V-8, I-5, PP:375-381, 2016.
- [9] Kumaravel A., Dutta P., Application of Pca for context selection for collaborative filtering, Middle - East Journal of Scientific Research, V-20, I-1, PP:88-93, 2014.
- [10] Krishnamoorthy P., Jayalakshmi T., Preparation, characterization and synthesis of silver nanoparticles by using phyllanthusniruri for the antimicrobial activity and cytotoxic effects, Journal of Chemical and Pharmaceutical Research, V-4, I-11, PP:4783-4794, 2012.

- [11] Amir M., Gungunes H., Slimani Y., Tashkandi N., El Sayed H.S., Aldakheel F., Sertkol M., Sozeri H., Manikandan A., Ercan I., Baykal A., Mössbauer Studies and Magnetic Properties of Cubic CuFe<sub>2</sub>O<sub>4</sub> Nanoparticles, *Journal of Superconductivity and Novel Magnetism*, V-32, I-3, PP:557-564, 2019.
- [12] Raj M.S., Saravanan T., Srinivasan V., A modified direct torque control of induction motor using space vector modulation technique, *Middle - East Journal of Scientific Research*, V-20, I-11, PP:1572-1574, 2014.
- [13] Khanaa V., Thooyamani K.P., Using triangular shaped stepped impedance resonators design of compact microstrip quad-band, *Middle - East Journal of Scientific Research*, V-18, I-12, PP:1842-1844, 2013.
- [14] Asiri S., Sertkol M., Güngüneş H., Amir M., Manikandan A., Ercan I., Baykal A., The Temperature Effect on Magnetic Properties of NiFe<sub>2</sub>O<sub>4</sub> Nanoparticles, *Journal of Inorganic and Organometallic Polymers and Materials*, V-28, I-4, PP:1587-1597, 2018. Thaya R., Malaikozhundan B., Vijayakumar S., Sivakamavalli J., Jeyasekar R., Shanthi S., Vaseeharan B., Ramasamy P., Sonawane A., Chitosan coated Ag/ZnO nanocomposite and their antibiofilm, antifungal and cytotoxic effects on murine macrophages, *Microbial Pathogenesis*, V-100, PP:124-132, 2016.
- [15] Kolanthai E., Ganesan K., Epple M., Kalkura S.N., Synthesis of nanosized hydroxyapatite/agarose powders for bone filler and drug delivery application, *Materials Today Communications*, V-8, PP:31-40, 2016.
- [16] Thilagavathi P., Manikandan A., Sujatha S., Jaganathan S.K., Antony S.A., Sol-gel synthesis and characterization studies of NiMoO<sub>4</sub> nanostructures for photocatalytic degradation of methylene blue dye, *Nanoscience and Nanotechnology Letters*, V-8, I-5, PP:438-443, 2016.
- [17] Thamotharan C., Prabhakar S., Vanangamudi S., Anbazhagan R., Anti-lock braking system in two wheelers, *Middle - East Journal of Scientific Research*, V-20, I-12, PP:2274-2278, 2014.
- [18] Thamotharan C., Prabhakar S., Vanangamudi S., Anbazhagan R., Coomasamy C., Hydraulic rear drum brake system in two wheeler, *Middle - East Journal of Scientific Research*, V-20, I-12, PP:1826-1833, 2014.
- [19] Vanangamudi S., Prabhakar S., Thamotharan C., Anbazhagan R., Collision control system in cars, *Middle - East Journal of Scientific Research*, V-20, I-12, PP:1799-1809, 2014.
- [20] Vanangamudi S., Prabhakar S., Thamotharan C., Anbazhagan R., Drive shaft mechanism in motor cycle, *Middle - East Journal of Scientific Research*, V-20, I-12, PP:1810-1815, 2014.
- [21] Anbazhagan R., Prabhakar S., Vanangamudi S., Thamotharan C., Electromagnetic engine, *Middle - East Journal of Scientific Research*, V-20, I-3, PP:385-387, 2014.
- [22] Kalaiselvi V.S., Prabhu K., Ramesh M., Venkatesan V., The association of serum osteocalcin with the bone mineral density in post menopausal women, *Journal of Clinical and Diagnostic Research*, V-7, I-5, PP:814-816, 2013.
- [23] Kalaiselvi V.S., Saikumar P., Prabhu K., Prashanth Krishna G., The anti Mullerian hormone-a novel marker for assessing the ovarian reserve in women with regular menstrual cycles, *Journal of Clinical and Diagnostic Research*, V-6, I-10, PP:1636-1639, 2012.
- [24] Thanigai Arul K., Manikandan E., Ladchumananandasivam R., Maaza M., Novel polyvinyl alcohol polymer based nanostructure with ferrites co-doped with nickel and cobalt ions for magneto-sensor application, *Polymer International*, V-65, I-12, PP:1482-1485, 2016.
- [25] Das M.P., Kumar S., An approach to low-density polyethylene biodegradation by *Bacillus amyloliquefaciens*, *3 Biotech*, V-5, I-1, PP:81-86, 2015.
- [26] Vanangamudi S., Prabhakar S., Thamotharan C., Anbazhagan R., Turbo charger in two wheeler engine, *Middle - East Journal of Scientific Research*, V-20, I-12, PP:1841-1847, 2014.
- [27] Vanangamudi S., Prabhakar S., Thamotharan C., Anbazhagan R., Design and calculation with fabrication of an aero hydraulic clutch, *Middle - East Journal of Scientific Research*, V-20, I-12, PP:1796-1798, 2014.
- [28] Saravanan T., Raj M.S., Gopalakrishnan K., VLSI based 1-D ICT processor for image coding, *Middle - East Journal of Scientific Research*, V-20, I-11, PP:1511-1516, 2014.
- [29] Ajona M., Kaviya B., An environmental friendly self-healing microbial concrete, *International Journal of Applied Engineering Research*, V-9, I-22, PP:5457-5462, 2014.
- [30] Hemalatha R., Anbuselvi S., Physicochemical constituents of pineapple pulp and waste, *Journal of Chemical and Pharmaceutical Research*, V-5, I-2, PP:240-242, 2013.
- [31] Langeswaran K., Revathy R., Kumar S.G., Vijayaprakash S., Balasubramanian M.P., Kaempferol ameliorates aflatoxin B<sub>1</sub> (AFB<sub>1</sub>) induced hepatocellular carcinoma through modifying metabolizing enzymes, membrane bound ATPases and mitochondrial TCA cycle enzymes, *Asian Pacific Journal of Tropical Biomedicine*, V-2, I-3 SUPPL., PP:S1653-S1659, 2012.
- [32] Masthan K.M.K., Aravindh Babu N., Dash K.C., Elumalai M., Advanced diagnostic aids in oral cancer, *Asian Pacific Journal of Cancer Prevention*, V-13, I-8, PP:3573-3576, 2012.

- [33] Asiri S., Güner S., Demir A., Yildiz A., Manikandan A., Baykal A., Synthesis and Magnetic Characterization of Cu Substituted Barium Hexaferrites, *Journal of Inorganic and Organometallic Polymers and Materials*, V-28, I-3, PP:1065-1071, 2018.
- [34] Vellayappan M.V., Jaganathan S.K., Manikandan A., Nanomaterials as a game changer in the management and treatment of diabetic foot ulcers, *RSC Advances*, V-6, I-115, PP:114859-114878, 2016.
- [35] Vellayappan M.V., Venugopal J.R., Ramakrishna S., Ray S., Ismail A.F., Mandal M., Manikandan A., Seal S., Jaganathan S.K., Electrospinning applications from diagnosis to treatment of diabetes, *RSC Advances*, V-6, I-87, PP:83638-83655, 2016.
- [36] Bavitra K., Sinthuja S., Manoharan N., Rajesh S., The high efficiency renewable PV inverter topology, *Indian Journal of Science and Technology*, V-8, I-14, 2015.
- [37] Vanangamudi S., Prabhakar S., Thamotharan C., Anbazhagan R., Design and fabrication of dual clutch, *Middle - East Journal of Scientific Research*, V-20, I-12, PP:1816-1818, 2014.
- [38] Sandhiya K., Kaviya B., Safe bus stop location in Trichy city by using gis, *International Journal of Applied Engineering Research*, V-9, I-22, PP:5686-5691, 2014.
- [39] Selva Kumar S., Ram Krishna Rao M., Deepak Kumar R., Panwar S., Prasad C.S., Biocontrol by plant growth promoting rhizobacteria against black scurf and stem canker disease of potato caused by *Rhizoctonia solani*, *Archives of Phytopathology and Plant Protection*, V-46, I-4, PP:487-502, 2013.
- [40] Sharmila S., Jeyanthi Rebecca L., GC-MS Analysis of esters of fatty acid present in biodiesel produced from *Cladophora vagabunda*, *Journal of Chemical and Pharmaceutical Research*, V-4, I-11, PP:4883-4887, 2012.
- [41] Arputhamary, B., & Arockiam, L. (2015). Data Integration in Big Data Environment. *Bonfring International Journal of Data Mining*, 5(1), 01-05.
- [42] Meymari, B.K., Mofrad, R.F., & Nasab, M.S. (2015). High Dynamic Range Receiver System Designed for High Pulse Repetition Frequency Pulse Radar. *International Academic Journal of Innovative Research*, 2(9), 1-20.
- [43] Abinaya, R., Abinaya, R., Vidhya, S., & Vadivel, S. (2014). Latent Palm Print Matching Based on Minutiae Features for forensic Applications. *International Journal of Communication and Computer Technologies*, 2(2), 85-87.
- [44] Dr. Krishnapriya, G. (2017). Identification of Money Laundering based on Financial Action Task Force Using Transaction Flow Analysis System. *Bonfring International Journal of Industrial Engineering and Management Science*, 7(1), 01to04.
- [45] Vakilfard, M., Taheri, A., & Salehifar, M.R. (2014). Implementation of the Satellite Ground Station Control in Real-Time Under Windows. *International Academic Journal of Science and Engineering*, 1(1), 1-9.
- [46] Aarthi, S., & Vijay, N. (2014). Sophisticated Data Entry Application using Matchmaking Algorithm through Scanned Images. *International Journal of System Design and Information Processing*, 2(1), 27-29.
- [47] Patidar, H.P., & Sharma, N. (2016). Adaptive Approach of DSR and OLSR Routing Protocols Using Optimal Probabilistic Logical Key Hierarchy in MANET. *Bonfring International Journal of Networking Technologies and Applications*, 3(2), 13-20.
- [48] Venkateswara Rao, B., and Nagesh Kumar, G.V. (2014). Voltage Collapse Proximity Indicator based Placement and Sizing of Static VAR Compensator using BAT Algorithm to Improve Power System Performance. *Bonfring International Journal of Power Systems and Integrated Circuits*, 4(3), 31-38.
- [49] Neenu Preetam, I., & Gupta, H. (2014). Cardless Cash Access using Biometric ATM Security System. *International Scientific Journal on Science Engineering & Technology*, 17(10), 893-897.
- [50] Revathi, M., Prakash, K., & Suguna, R. (2018). A Systematic Study on Cyber Physical System. *Bonfring International Journal of Research in Communication Engineering*, 8(1), 1-4.